Pressure and Cooling Rate-Induced Densification of Atactic Polystyrene

Roberto Pantani

Department of Chemical and Food Engineering, University of Salerno, via Ponte don Melillo, I-84084 Fisciano (SA), Italy

Received 11 April 2002; accepted 25 September 2002

ABSTRACT: The exact knowledge of postprocessing polymer-specific volume is often a factor of enormous strategic importance from an industrial point of view. The subject is complicated by the fact that the specific volume of solid polymers at a constant temperature and pressure is not only a function of the current temperature and pressure, but is also a consequence of the whole formation history from the melt. In this work, specific volumes of samples solidified in different conditions are analyzed and related to their formation history. A wide range of cooling rates (from 5 $\times 10^{-3}$ to 300 K/s) and solidification pressures (from 0.1 to 80 MPa) are examined. The results show a synergic effect of the cooling rate and solidification pressure: Lower cooling rates result in a much higher pressure-induced densification with respect to higher cooling rates. A simple phenomenological model which essentially links the densification effect to the dependence of the glass transition temperature upon the cooling rate and solidification pressure is adopted to describe the experimental data. Starting from the densification effect, the effect of the pressure and cooling rate on the glass transition temperature is evaluated. Furthermore, some conclusions about the dependence of the volume relaxation time on the temperature and pressure in the glass transition range are achieved. © 2003 Wiley Periodicals, Inc. J Appl Polym Sci 89: 184–190, 2003

Key words: polystyrene; density; glass transition

INTRODUCTION

The specific volume of amorphous polymers as a function of the temperature and pressure is often described by equations of state, like, for instance, the Tait equation[1] or the Spencer–Gilmore equation,[2] which represent a valuable mean to determine the volumetric properties at a first level of approximation. Equations of this kind are quite accurate as far as the molten polymer is concerned. However, many literature results[3–10] show that the specific volume in the glassy state is determined by the whole formation history and not only by the current temperature and pressure. This obviously means that equations of state are inadequate for the description of a solid polymer volume after a given thermomechanical history if higher degrees of accuracy are needed. From a practical point of view, the exact knowledge of postprocessing specific volume can be of enormous strategic importance in industry, since dimensional accuracy is often one of the most important factors determining plastic product quality.[11]

McKinney and Simha[4] showed that, if no volume relaxation is present below the T_g, equations of state can still be used to derive all relevant thermodynamic parameters (thermal expansion, volume compressibility) also in the solid state: The pressure-induced densification phenomenon is, in fact, due mainly to the dependence of the glass transition temperature upon the pressure. Since, based on Kovacs'[10] and Greiner and Schwarzl's results,[12] among others, the glass transition temperature is also dependent upon the cooling rate. By the same reasoning, the densification induced by low cooling rates can also be interpreted.

In this work, a specific volume of samples solidified in different conditions are analyzed and related to their formation history. In particular, the combined effects of several cooling rates and solidification pressures are considered. Starting from the assumption of no relaxation below the T_g, the densification phenomenon is related to the dependence of the glass transition temperature on the particular thermomechanical history through a simple phenomenological equation.

EXPERIMENTAL

Materials

An atactic polystyrene (Dow PS678E, M_w = 250,000, M_w/M_n = 2.9), previously characterized as far as most of the properties of interest for this work,[11–14] was adopted for all the experiments. A DSC cooling ramp (performed using a Mettler DSC apparatus (Griefensee, Switzerland) under a nitrogen-flowing atmosphere) at a cooling rate of 0.2 K/s is reported in

Correspondence to: R. Pantani (rpantani@unisa.it).

Journal of Applied Polymer Science, Vol. 89, 184–190 (2003)

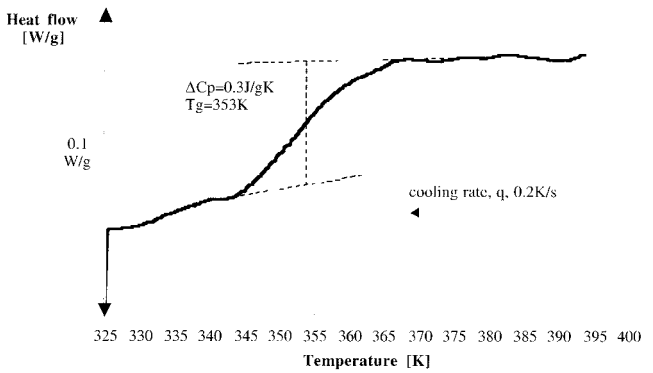

Figure 1 DSC cooling ramp of DOW PS678E at a rate of 0.2 K/s.

Figure 1. At this cooling rate, the glass transition temperature can be evaluated as T_g = 353 K (close to that reported by Douven et al.[14] for the same material), and the difference between the melt and solid heat capacities as $\Delta Cp = 0.3\ \mathrm{J\ g^{-1}\ K^{-1}}$.

The material PVT behavior in equilibrium conditions was taken from C-Mold 99.1 of the AC Technology database. The C-Mold data base[11] refers to a characterization procedure based on isothermal compression–volume change measurements starting at each temperature from room pressure. The PVT behavior explored, as specified above, was described by AC Technology using the following modified form of the Tait equation[11]:

$$v(T, P) = v_0(T)\left\{1 - C\ \ln\left[1 + \frac{P}{B(T)}\right]\right\} \qquad (1)$$

with $C = 0.0894$ and

	if $T > T_r(P)$	if $T < T_r(P)$
$v_0(T) =$	$B1m + B2mT_c$	$B1s + B2sT_c$
$B(T) =$	$B3m \exp(-B4mT_c)$	$B3s \exp(-B4sT_c)$
$T_c =$	$T - B5$	
$T_r(P) =$	$B5 + B6P$	

The values of the parameters to be used in eq. (1) for Dow PS 678E are listed in Table I.

Densification experiments

Three different methods were used to induce sample densification:

1. Treatments inside the confined fluid cell whose temperature and pressure could be controlled.
2. Solidification in a DSC apparatus under a constant cooling rate;
3. Quenching of films at room pressure while a careful measurement of the thermal history was performed.

As far as the first series of experiments, cylindrical samples (height, 1 mm; diameter 2.5 mm) were prepared for treatments inside the oil cell, which was already described elsewhere[15]; the initial treatment of 20 min at 453 K followed by slow cooling to room temperature was adopted to erase the effect of previous histories. The samples subjected to this initial treatment were used as a starting point for further treatments in the oil cell. After the initial treatment, the samples were vacuum-sealed in a DuPont Teflon PFA bag to prevent the plasticizing effect of the oil and kept for 30 min at 403 K and under a constant pressure (ranging from 0.1 to 80 MPa) inside the oil cell. The treatment pressure was kept constant also during the whole cooling (at a cooling rate ranging from 0.1 to 2.5 K/s, depending on the coolant flow rate inside the cooling channels) from 403 to 296 K. The second series of experiments was performed using a DSC apparatus (Mettler, with liquid nitrogen as the cooling fluid), by which samples were kept at 453 K for 20 min and then solidified at room pressure with constant cooling rates ranging in the interval 5×10^{-3} to 1.7 K/s.

For the third series of experiments, films having a thickness of 100 μm, produced by compression molding, were kept at 403 K for 20 min in the quenching apparatus already described elsewhere[16] and then cooled to room temperature. Consistently with the quenching procedure, the cooling rate is determined by the temperature difference between the sample and the cooling medium and, thus, decreased during the test with a decreasing temperature. The cooling rate at the temperature of 353 K, that is, at the T_g measured by DSC as shown in Figure 1, was chosen as being representative of the quenching effectiveness. According to this choice, the obtained cooling rates ranged from 0.1 to 300 K/s depending on the flow rate and on the nature of the cooling medium (air or water). Two more samples were cooled in the temperature-controlled chamber of the same apparatus at much slower cooling rates (3×10^{-3} and 0.02 K/s).

TABLE I
Values of Parameters Appearing in Eq. (1), as Taken From C-Mold99.1 Database, Describing the Equilibrium PVT Behavior of Dow PS 678E

Parameter	Values
$B1m$ (m^3/kg)	0.976×10^{-3}
$B2m$ (m^3, kg^{-1} K^{-1})	5.93×10^{-7}
$B3m$ (Pa)	1.71×10^{8}
$B4m$ (1/K)	3.88×10^{-3}
$B1s$ (m^3/kg)	0.976×10^{-3}
$B2s$ (m^3 kg^{-1} K^{-1})	2.32×10^{-7}
$B3s$ (Pa)	2.5×10^{8}
$B4s$ (l/K)	3.6×10^{-3}
$B5$ (K)	368.15
$B6$ (K/Pa)	3.6×10^{-7}

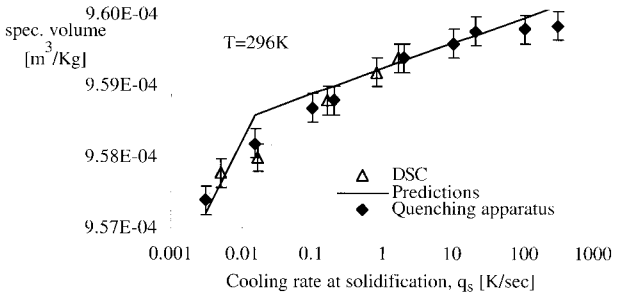

Figure 2 Cooling rate-induced densification. Full line refers to predictions obtained by eq. (4) with T_g expressed by eq. (9).

Density measurements

All sample densities were measured using density-gradient columns of NaCl and water kept at 296 K. The density data shown in this work were measured 30 min after the end of the solidification procedure (i.e., starting from the instant at which the sample reached room temperature). During this time, the effect of the volume relaxation at room pressure can be considered negligible.[17]

The resolution of the density-gradient columns was about 10^{-8} m^3/kg. The reproducibility of the specific volume after treatments is, however, about 10 times larger. Thus, in the following, specific volume data after treatments are reported with error bars of $\pm 2 \times 10^{-7}$ m^3/kg.

RESULTS

The densification effect of the cooling rate on samples solidified at room pressure (using DSC and quenching apparatus) is shown in Figure 2. The data collected with the quenching apparatus fall on the same curve as that described by samples obtained by DSC which experienced a constant cooling rate, thus confirming that the cooling rate at 353 K (i.e., approximately at the T_g), referred to as q_s in the following, is indeed representative of the whole cooling history effectiveness.

As expected, higher cooling rates result in higher specific volumes. The dependence is about linear on a semilog plot. If the densification effect is described by the relationship

$$\alpha' = \frac{1}{v}\frac{\partial v}{\partial \log\left(q_s \frac{s}{K}\right)} \tag{2}$$

from data reported in Figure 1, α' for solidifications under room pressure can be calculated as 0.05% per decade, in good agreement with the data reported by Kogoski and Filisko[7] for an aPS with M_w = 310,000, showing an α = 0.04% per decade.

Pressure-induced densification for samples solidified in the oil-filled cell is shown in Figure 3 for each series of data, characterized by different cooling rates; a higher solidification pressure, P_s, results in a lower sample volume, with a fairly linear relationship [Fig. 3(a)]. The effect of the cooling rate is clearly shown also for data presented in Figure 3: At each solidification pressure, a higher cooling rate induces a higher specific volume [Fig. 3(b)].

If, according to McKinney and Simha,[4] the densification effect can described by the pseudocompressibility

$$\beta' = -\frac{1}{v}\frac{\partial v}{\partial P_s} \tag{3}$$

from the data reported in Figure 3; β' can be calculated as 9×10^{-5} MPa^{-1} for samples solidified by a low cooling rate (0.1 K/s), in agreement with the value reported by McKinney and Simha[4] and close to other values reported in the literature. For an aPS with M_w = 30,000, Greener[8] found a value of 7.7×10^{-5} MPa^{-1} for a cooling rate of 0.02 K/s; a similar result was found by Oels and Rehage[5] (7.5×10^{-5} MPa^{-1}) for an aPS with M_w = 20,000 at a cooling rate of 0.05 K/s.

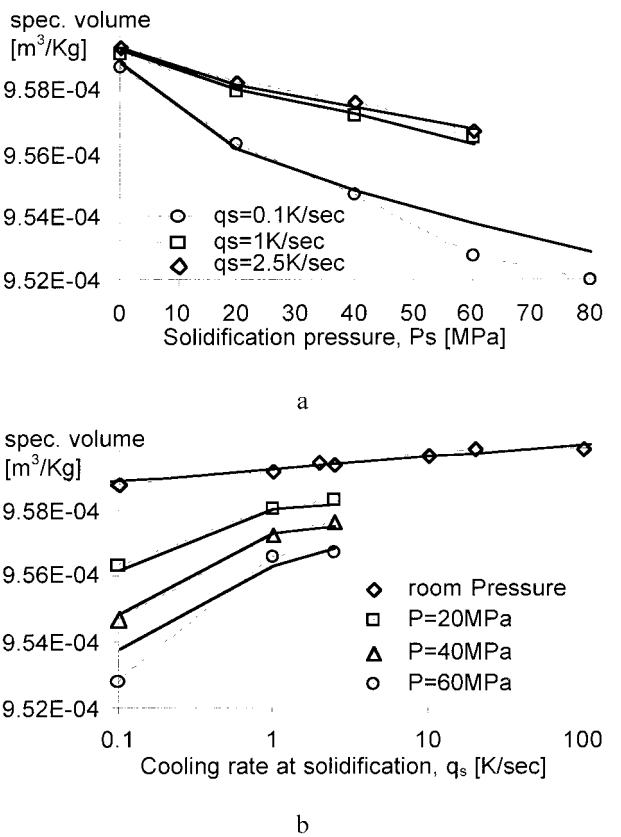

Figure 3 Pressure-induced densification. Full lines refer to predictions obtained by eq. (4) with T_g expressed by eq. (9).

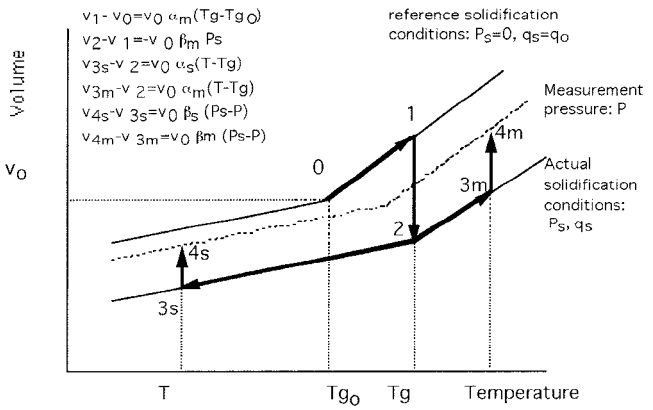

Figure 4 Steps followed to obtain the specific volume of an amorphous polymer solidified at given pressures and cooling rates.

However, for higher cooling rates (namely, 1 and 2.5 K/s), the data reported in Figure 3 show that β' is much lower (4.5×10^{-5} MPa^{-1}). There seems, therefore, to be a synergic effect of the pressure and cooling rate on the densification: Lower cooling rates result in a much higher pressure-induced densification with respect to higher cooling rates [Fig. 3(b)].

DISCUSSION

To describe the specific volume after solidification under pressure at different cooling rates, following the approach suggested by McKinney and Simha,[4] the following phenomenological equation can be proposed:

$$v(P, T, q_s, P_s) = v_0[1 + (\alpha_m - \alpha_i)(T_g - T_{g0}) - (\beta_m - \beta_i)P_s + \alpha_i(T - T_{g0}) - \beta_i P] \quad (4)$$

where P and T are the current pressure and temperature, respectively; T_g, the actual glass transition temperature (function of the solidification pressure and cooling rate); P_s and q_s, the pressure and cooling rate during solidification (namely, when glass transition takes place); T_{g0}, the glass transition temperature at room pressure and at a reference cooling rate; v_0, the specific volume at $T = T_{g0}$ and $P = 0$; and α_m and β_m, the thermal expansion coefficient and compressibility of the molten polymer, respectively. α_i and β_i stand for the thermal expansion coefficient and compressibility, respectively, and refer to the melt (subscript "i" = "m") if $T > T_g$ and to a solid (subscript "i" = "s") if $T < T_g$.

Equation (4) is easily obtained by summing up the contributions of the steps represented in Figure 4 and, as mentioned above, relies on the hypothesis that no volume relaxation or material structural modification occurs below the T_g. Obviously, this hypothesis will be verified only if residence times at each temperature below the T_g are short with respect to the material volume relaxation times.

Through eq. (4), densification effects due to the cooling rate and solidification pressure are easily accounted for:

$$\alpha' = \frac{1}{v_0}\left.\frac{\partial v}{\partial \log\left(q_s \frac{s}{K}\right)}\right|_{\text{const. } T \text{ and } P} = \left.\frac{\partial T_g}{\partial \log\left(q_s \frac{s}{K}\right)}\right|_{P=P_s} (\alpha_m - \alpha_s)$$

$$\beta' = -\frac{1}{v_0}\left.\frac{\partial v}{\partial P_s}\right|_{\text{const. } T \text{ and } P} = -\left.\frac{\partial T_g}{\partial P_s}\right|_{q=q_s} (\alpha_m - \alpha_s) + (\beta_m - \beta_s) \quad (5)$$

and essentially relate both phenomena to the dependence of the glass transition temperature on the cooling rate and pressure. It could be worth noticing that if T_g is taken as the intersection of volume curves of the solid and melt at each pressure, as normally done when PVT measurements in equilibrium conditions are performed,[18] that is,

$$T_g(P_s) = T_{g_0} + \frac{\beta_m - \beta_s}{\alpha_m - \alpha_s} P_s \quad (6)$$

eqs. (5) do not predict any densification and eq. (4) becomes an equation of state like eq. (1).

The parameters in eq. (4) are easily obtained from the data reported above: Following the approach suggested by McKinney and Simha,[4] thermal expansion coefficients and volume compressibilities can be obtained from the Tait equation with the parameters reported in Table I. T_{g0} was taken as 353 K, as measured during the DSC cooling ramp at 0.2 K/s reported in Figure 1; the value of the parameter v_0 was appropriately chosen to describe by eq. (4) the specific volume at room temperature and pressure of the sample solidified by DSC at a rate of 0.2 K/s (reported in Fig. 2). The values adopted for the parameters in eq. (4) are listed in Table II.

TABLE II
Values Adopted for Parameters in Eq. (4)

Parameter	Value
V_0 (m^3/kg)	0.9718×10^{-3}
T_{g0} (K)	353
α_m (1/K)	5.16×10^{-4}
β_m (1/MPa)	5.00×10^{-4}
α_S (1/K)	2.28×10^{-4}
β_S (1/MPa)	3.21×10^{-4}

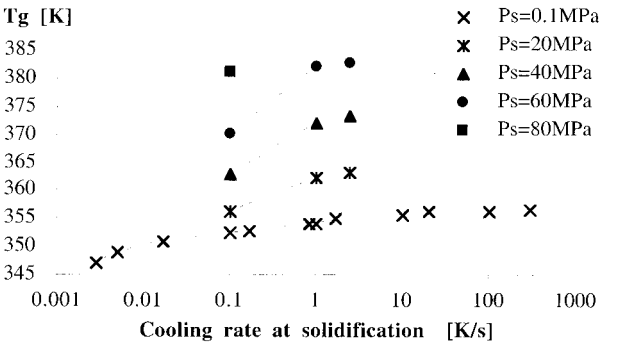

Figure 5 Dependence of glass transition temperature [as predicted by eq. (4), on the basis of specific volume data presented in Figs. 2 and 3] on the cooling rate and solidification pressure.

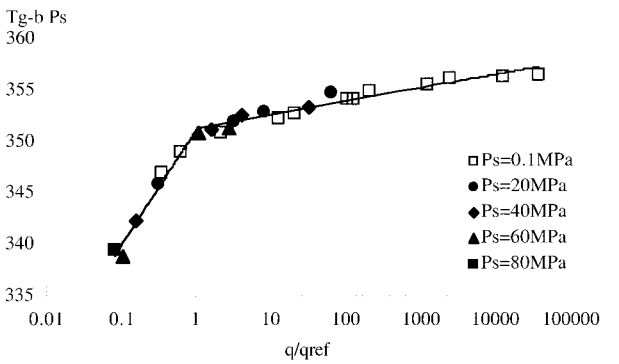

Figure 6 Master curve for T_g. Data are corrected for pressure effect and reported versus a fictitious cooling rate obtained by dividing the real cooling rate by a shift factor, a function of the solidification pressure.

Using the experimentally measured values of α' and β' presented in the Experimental section above and the values of α and β reported in Table II, one obtains from eq. (5) that $T_g/\partial\log(q_s) = 1.7$ K/decade (under room pressure), which is about the same result found by DSC analysis,[15] and that $\partial T_g/\partial P_s = 0.31$–$0.47$ K/MPa (depending on the cooling rate), which is of the same order of magnitude as that of the result suggested by Clapeyron's equation:

$$\frac{\partial T_g}{\partial P_s} = \frac{v_0 T_{g_0}(\alpha_m - \alpha_s)}{\Delta C_p} = 0.4 \text{ K/MPa} \qquad (7)$$

and very close to the results reported by Schneider.[19] Equation (6) would provide a much higher value: $\partial T_g/\partial P_s = 0.62$ K/MPa, stressing the inadequacy of applying an equation of state when high degrees of accuracy are needed.

Supposing the validity of eq. (4) for each of the tests presented in this work, this equation can be adopted to calculate the glass transition temperature during a particular solidification history by imposing the resulting specific volume [v in eq. (4)] and finding the corresponding value of T_g. Each of the specific volumes presented in Figures 2 and 3 corresponds, thus, through eq. (4), to a glass transition temperature. The results of this procedure, adopting the parameters listed in Table II, are shown in Figure 5, where T_g is reported versus the cooling rate for the five solidification pressures applied in this work. According to the results reported in Figure 5, the glass transition temperature seems to depend almost linearly on the log of the cooling rate at each solidification pressure (in agreement with Greiner and Schwarzl's results[12]); however, the slope of the plots is strongly dependent on the pressure.

A master-curve approach can be attempted on the data reported in Figure 5 by adopting the following variables:

$$T_g - bP_s = \text{function of } \ln[q_s/q_{\text{ref}}(P_s)], \quad \text{with} \quad q_{\text{ref}}(P_s) = d(1 + cP_s) \qquad (8)$$

The results of this change of variables are shown in Figure 6 and the values adopted for the constants are reported in Table III. All data, obtained in a wide range of cooling rates and solidification pressures, collapse onto the same curve, which at a first approximation can be described by two distinct lines, which intersect at a temperature $T_{gr} = 351$ K.

On the basis of this result, the following equation can be proposed for the dependence of the glass transition temperature on the combined effect of the cooling rate and pressure:

$$T_g = T_{g_{\text{ref}}}(P_s) + \frac{1}{a}\ln\left[\frac{q_s}{q_{\text{ref}}(P_s)}\right], \quad \text{with} \quad \begin{cases} T_{g_{\text{ref}}}(P_s) = T_{g_r} + bP_s \\ q_{\text{ref}}(P_s) = d(1 + cP_s) \\ a = a_L \quad \text{if} \quad q < q_{\text{ref}}(P_s) \\ a = a_H \quad \text{if} \quad q \geq q_{\text{ref}}(P_s) \end{cases} \qquad (9)$$

and the values found for the constants for the material adopted in this work are reported in Table III. Equation (8) differs from the commonly adopted equations found in the literature[6,8] which assume a linear dependence of the T_g upon $\ln(q)$ and P_s, essentially because

TABLE III
Values of the parameters to be adopted for Eq. 9 and 11

Parameter	Value
T_{g_r} (K)	352
a (1/K)	
a_L	0.26
a_H	1.89
b (K/MPa)	0.51
c (MPa^{-1})	2.41
d (K/s)	0.01

it introduces a change of slope (through the parameter "a") for the dependence upon the cooling rate at a reference cooling rate, q_{ref}, which, in turn, depends on the pressure.

Of course, if eq. (9), with the parameters reported in Table III, is adopted to describe the glass transition temperature, eq. (4) becomes predictive toward the specific volume after a given thermomechanical history. The results obtained for the tests presented in this work are reported in Figures 2 and 3.

Free-volume theory and relaxation time

According to kinetic theories (as, for instance, the KAHR model[20]), the glass transition is a purely kinetic phenomenon which appears when the response time for the system to reach equilibrium is of the same order as that of the timescale of the experiment.[21] If, in particular, the following simple equation is adopted to describe a specific volume change with the time at constant pressure,[22]

$$\frac{dv}{dt} = -\frac{v - v_e}{\tau} + \alpha * T' \tag{10}$$

(where v_e is the equilibrium volume, a function of the temperature and pressure, α^* accounts for the instantaneous response of the volume to a sudden change in temperature, and τ is the effective relaxation time in the sense introduced by Kovacs[10]), the glass transition temperature can also be interpreted as the temperature T at which the specific volume v separates from its equilibrium value during cooling. This happens when the Deborah number, defined as the ratio between the observation timescale (in our case, equal to $1/q$) and the timescale of the system ($-d\tau/dT$) becomes equal to 1. If the activation energy, E_a, is defined as

$$E_a = R\left[\frac{d\ \ln(\tau)}{d1/T}\right]_T \tag{11}$$

where R is the ideal gas constant, the Deborah number can be written as

$$D(T) = \frac{E_a}{RT^2}\, q\tau \tag{12}$$

and, thus, at the glass transition temperature,

$$q_s\tau = D(T_g)\,\frac{RT_g^{\,2}}{E_a} \tag{13}$$

With the ratio $E_a/(R\ T_g^{\,2})$ often found not far from 0.5 (ref. 23), at the glass transition temperature, the product $\tau \bullet q$ becomes equal to a constant k of about 2 K, that is, $\tau = k/q$. After eq. (9), it can thus be written

$$\frac{\tau}{k} = \frac{1}{d(1 + cP_s)}\exp[-a(T - T_{g_{ref}})],$$

$$\text{with} \quad \begin{cases} T_{g_{ref}}(P_s) = T_{g_{ref}} + bP_s \\ a = a_L \quad \text{if} \quad T < T_{g_{ref}}(P_s) \\ a = a_H \quad \text{if} \quad T \geq T_{g_{ref}}(P_s) \end{cases} \tag{14}$$

Equation (14) describes the effect of the pressure and temperature on the volume relaxation time at temperatures close to the glass transition and (as shown in Fig. 7) indicates that

- At constant pressure, the relaxation time decreases exponentially with increasing temperature;
- At a constant temperature, with increasing pressure, a general increase of the relaxation time takes place. However, this is a result of two counteracting mechanisms: relaxation phenomena accelerate because the preexponential term in eq. (14) decreases; on the other hand, the exponential term increases (an increasing pressure acts like a temperature shift downward). The second mechanism can be interpreted as a reduction of the free

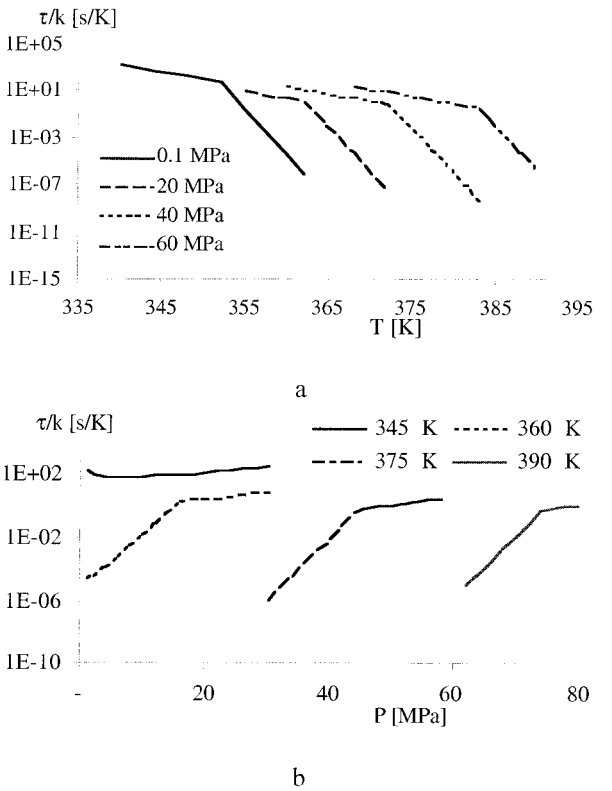

Figure 7 Dependence of the volume relaxation time (a) on the temperature for several pressures and (b) on the pressure for several temperatures, as described by eq. (14) with parameters listed in Table III ($k \approx 2$ K).

volume. The first mechanism is generally overcome by the second one and, thus, the neat effect is that the relaxation time increases exponentially with increasing pressure except at low pressures and temperatures, where the pressure, according to eq. (14), seems even to induce a faster relaxation (Fig. 7). Indeed, eqs. (9) and (14) should be interpreted as linearizations of more complex Vogel- or Arrhenius-type expressions, and their accuracy far beyond the range (in terms of temperatures and cooling rates) examined in this work should be further investigated.

There is a scarcity of data in the literature about the effect of pressure on the volume relaxation in solid polymers. Tribone et al.[24] performed a series of measurements on an aPS with M_w = 30,000. They found an exponential increase of the relaxation time with the pressure of the same order as that described by eq. (14). In particular, Tribone et al.[24] reported an increase of the relaxation time for solid aPS at a rate of about 1 decade/30 MPa, whereas eq. (14) predicts about 1 decade/20 MPa. The reported effect of the temperature on the relaxation time for solid aPS (ref. 24) is the same as that described by eq. (14), that is, the relaxation time for solid aPS decreases at a rate of about 1 decade/9 K.

An interesting feature of eq. (14) is that it indicates that the relaxation time presents a weaker dependence on the temperature for temperatures below the $T_{g\mathrm{ref}}$ (P_s) (Fig. 7). This change in the slope was recently pointed out by Simon et al.[25] who collected data at room pressure from several literature works on PS and noticed that, for temperatures below the T_g, the temperature dependence of the relaxation time appears to be significantly weaker. The data reported in this work indicate that this change in slope is present at all pressures at a reference glass transition temperature which depends on the solidification pressure. This feature of the relaxation time is of major importance, since the exact knowledge of the volume relaxation below the T_g is critical for accurate predictions of relaxation phenomena; neglecting this phenomenon, for instance, by extrapolating data referring to the melt, can lead to an overestimation of the relaxation time by orders of magnitude.

CONCLUSIONS

Experimental determinations of the cooling rate and pressure-induced densification on an amorphous polystyrene were conducted by measuring the specific volumes of samples solidified with several formation histories. The results show that both the cooling rate and pressure induce a relevant densification and that the effects are synergic: Lower cooling rates result in higher values of pseudocompressibility with respect to higher cooling rates.

Starting from the assumption that the densification phenomenon is essentially due to the dependence of the glass transition temperature on the particular thermomechanical history, a simple phenomenological equation was applied to calculate the glass transition temperature during each solidification test starting from the final sample volumes. An equation relating the glass transition temperature to the combined effects of the cooling rate and pressure was thus achieved. This equation presents a change of the slope for the dependence upon the cooling rate at a reference temperature (which depends on the pressure). If this equation is interpreted by applying a classical formulation of the free-volume theory, the result provides an expression for the dependence of the volume relaxation time upon the temperature and pressure in the glass transition range and indicates that the relaxation time presents a weaker dependence on the temperature for temperatures below a reference glass transition temperature (which, in turn, depends on the pressure). This feature of the relaxation time is of major importance to obtain accurate predictions of relaxation phenomena: If this phenomenon is neglected, for instance, by extrapolating data referring to the melt, the volume relaxation time below the T_g can be overestimated by orders of magnitude.

References

1. Zoller, P.; Hoehn, H. H. J Polym Sci Polym Phys Ed 1982, 20, 1385.
2. Spencer, R. S.; Gilmore, G. D. J Appl Phys 1950, 21, 523.
3. Shishkin, N. I. Sov Phys Solid State 1960, 2, 350.
4. McKinney, J. E.; Simha, R. J Res Natl Bur Stand A 1977, 81, 283.
5. Oels, H.-J.; Rehage, G. Macromolecules 1977, 10, 1036.
6. Yu, J. S.; Lim, M.; Kalyon, D. M. Polym Eng Sci 1991, 31, 145.
7. Kogowski, G. J.; Filisko, F. E. Macromolecules 1986, 19, 828.
8. Greener, J. Polym Eng Sci 1986, 26, 534.
9. Colucci, D. M.; McKenna, G. B.; Filliben, J. J.; Lee, A.; Curliss, D. B.; Bowman, K. B.; Russell, J. D. J Polym Sci B Polym Phys 1997, 35, 1561.
10. Kovacs, A. J. Fortschr Hochpolym Forsch 1964, 3, 394.
11. C-Mold 99.1 User's guide, SHRINKAGE & WARPAGE; pp 2–5.
12. Greiner, R.; Schwarzl, F. R. Rheol Acta 1984, 23, 378.
13. Flaman, A. A. M. Ph.D. Thesis, Tueindhoven, NL, 1990.
14. Douven, L. F. A.; Baaijens, F. P. T.; Meijer, H. E. H. Prog Polym Sci 1995, 20, 403.
15. Pantani, R.; Titomanlio, G. Int J Form Process 1999, 2, 211.
16. Pantani, R.; Titomanlio, G. J Appl Polym Sci 2001, 81, 267.
17. Pantani, R.; Titomanlio, G., submitted for publication in J Polym Sci Polym Phys Ed.
18. McKenna, G. B. In Comprehensive Polymer Science, Vol. 2, Polymer Properties; Booth, C.; Price, C., Eds.; Pergamon: Oxford, 1989; Chapter 10.
19. Schneider, H. A. J Therm Anal 1996, 47, 453.
20. Kovacs, A. J.; Aklonis, J. J.; Hutchinson, J. M.; Ramos, A. R. J Polym Sci Polym Phys Ed 1979, 17, 1097.
21. Gedde, U. W. Polymer Physics; Chapman & Hall: London, 1995.
22. Hodge, I. M. J Non-Cryst Solids 1946, 29, 240.
23. Tool, A. Q. J Am Ceram Soc 1994, 169, 211.
24. Tribone, J. J.; O'Reilly, J. M.; Greener, J. J Polym Sci B Polym Phys 1989, 27, 837.
25. Simon, S. L.; Sobieski, J. W.; Plazek, D. J. Polymer 2001, 42, 2555.